**FACTA UNIVERSITATIS**
Series: **Electronics and Energetics** Vol. 38, Nº 2, June 2025, pp. 277 - 288
https://doi.org/10.2298/FUEE2502277K

**Original scientific paper**

# SELECTION OF MICRO WIND TURBINE BLADE DESIGN BASED ON SYMMETRIC NACA 4-DIGIT AIRFOILS

**Sanjay Kumar[1], Abhishek Verma[1], Yajvender Pal Verma[2], Amarjeet Singh[3]**

[1]Department of Electrical Engineering, University Institute Technology Himachal Pradesh University Shimla, India
[2]Department of Electrical Engineering, UIET, Punjab University Chandigarh, India
[3]Department of Computer Science, HPU Shimla

| | | |
|---|---|---|
| ORCID iDs: | Sanjay Kumar | https://orcid.org/0000-0002-9938-2111 |
| | Abhishek Verma | https://orcid.org/0009-0003-4327-8838 |
| | Yajvender Pal Verma | https://orcid.org/0000-0003-3192-4700 |
| | A. J. Singh | https://orcid.org/0009-0004-5352-3873 |

**Abstract**. *Wind power has become a key component for electrical power generation to develop sustainable energy sources. Empowered by the landmark NACA 1933 report on symmetric airfoils, this research paper sets out to revive a historical legacy in aerodynamics by measuring the impact of chord-wise thickness variations on the lift and drag characteristics of symmetric NACA 4-digit airfoils. This study aims to examine the performance of a micro wind turbine that has been expressly developed for rooftop application, where wind speeds are generally low. In the present study, 6 symmetrical designs of the air profile of NACA are taken. Then their characteristics like lift, drag lift and lift-to-drag ratio w.r.t. various angles of attacks have been compared for each profile using Xfoile Software. Finally, it was found the NACA 0025 at ReY No. $10^6$ offers the best lift of 90 with an angle of attack in range of -8.75°-10.7 & ratio of lift to drag is 68.9.*

**Key words**: *Wind turbine, Airfoils, aerodynamics, NACA, Wind speed.*

## 1. INTRODUCTION

The economic growth of any nation depends upon the use of energy. The world population is expected to reach 9.7 billion by 2050, resulting in a steady increase in energy consumption [1]. Energy markets began to tighten after post-COVID crisis scenarios. Several nations that are on the edge of a major recession, rising energy costs have hampered economic growth, pushed households into poverty. If comparing the recent energy crisis with the oil

Received September 18, 2024; revised December 22, 2024; accepted January 25, 2025
**Corresponding author**: Sanjay Kumar
Department of Electrical Engineering, University Institute Technology
Himachal Pradesh University, Shimla, India
E-mail: sanjnitham@gmail.com

shocks of the 1970, the difference is that today's crisis involves all fossil fuels [2]. Compared to fifty years ago, the global economy is now considerably more interconnected, which amplifies the impact. Because of this, it can be called the first really global energy crisis. Traditional energy sources such as oil, natural gas, and coal are the most effective drivers of economic growth, providing more than 80% of the energy consumption [3]. The environmental concerns, the depletion of fossil fuel reserves, energy price shocks, non-renewable features of oil, biogas, solid waste as energy sources and global warming have caused renewable energies to be considered as an alternative to traditional energy sources [4]. Renewable energy, a cornerstone of eco-friendly activities, encompasses various types like solar, geothermal, hydropower, biomass, ocean, tidal, wind, etc. that promise a cleaner energy future. Among them, solar energy stands out as a front-runner, tapping into the sun's abundant rays through photovoltaic technology [5]. Solar power not only offers a sustainable solution but also contributes to reducing reliance on traditional fossil fuels but the amount of solar energy that could be harnessed depends largely on three factors [6]: the first one is the time of the day, the second is the weather conditions, and the last one is the location, i.e., latitude and longitude. Thus, another solution for energy demand could be wind energy, which can be forecast at any time of the day [7]. With the advancement of technology and awareness throughout society, a shift can be seen. With more and more advancements in wind harnessing methods, wind turbines are used very frequently. The past three decades have given us remarkable improvements in wind turbine designs like Darrieus Turbine, Savonius Turbine, HAWT, etc., but all these focuses more on large-scale designs that could only be installed in remote locations or off-shore places. Less emphasis has been placed on small and micro-wind turbines that could be used for single-household purposes and are suitable for providing off-grid solutions to problems with proper study of location wind speed and design of the turbine. Micro wind turbine crucial part lies with its blade design that must directly face the wind to convert the kinetic energy of wind into mechanical motion thus moving the generator to produce electrical equivalent output. Blade design includes the choice of airfoil, optimization of chord length and torsion angle distribution, as well as determination of blade thickness to blade chord length [8]. The airfoil is a crucial component of wind turbine blades that must be taken into account during the design process. Otto Lilienthal's [9] work on aerodynamics laid some early foundations for understanding lift and airfoil shapes. The characteristics of 78 related airfoil sections from tests in the variable-density wind tunnel [10] discuss the effects of blade shape on wind turbine performance and are foundational for the field of airfoil sections specifically for wind turbine applications of symmetrical airfoil sections, which are relevant for vertical axis wind turbines (VAWTs) and horizontal axis wind turbines (HAWTs). S.S. Bhat [11] investigated oscillating NACA 0012 airfoils at low Reynolds Numbers around the stall angle and concluded that a leading-edge vortex is formed due to shear layer separation from the leading edge. Matyushenko [12] studied flow around various airfoils with different shapes and thicknesses using two-dimensional RANS. They found that while the lift coefficient is bigger than the experimental value for higher angles of attack, the computational results and experimental data agree well for modest angles of attack (up to 7–12°). Morgado [13] compared CFD and XFOIL performance predictions for high lift low Reynolds number airfoils and found that XFOIL results are as good as CFD results [11,13-15]. Many studies have considered Reynolds number, range [14-16], low surface roughness, better strength [17-19] cheap cost, and noise-free [20,21] character is desired for the design of wind turbine blades [22–24]. Lift-to-draper embarks on a journey to revisit and revitalize a historical legacy in aerodynamics using modern

tools to systematically investigate how chord-wise thickness variations influence the aerodynamic performance relevance of symmetric By evaluating the effects of chordwise thickness variations on the lift and drag characteristics of symmetric NACA 4-digit airfoils for a wide range of angles of attack and Reynolds numbers, this thorough computational investigation of NACA 4-digit airfoils aims to close the gap between historical insights and contemporary engineering practices, reflecting the complexity of real-world wind conditions. By quantifying the influence of thickness variations, endeavor to unearth specific profiles capable of consistently reducing drag and augmenting lift. In doing so, we hope to contribute to the continual evolution of wind turbine technology beyond theoretical significance.

## 2. METHODOLOGY

### 2.1. Optimum Airfoil Design Selection

The selection of airfoils for the blades of the micro wind turbine involves considering multiple steps shown in Fig. 1. To determine which airfoils have the highest Cp, a simulation has to be performed and run to build the micro wind turbine blades. The airfoils selected for this investigation have been developed specifically to perform well at low wind speeds. The performance of these airfoils at low Reynolds numbers, which correspond to the operating circumstances in the lower and middle portions of the Shivalik mountains of the Himalayas needs to be examined. The study of these airfoil designs, considering various aerodynamic and airfoil design characteristics is mainly performed using CFD analysis and simulation software [11]. A crucial factor in determining a constant for linking airflow characteristics is the Reynolds number. The investigation concentrated on low wind speeds, resulting in Reynolds number values of 3.0x10^4, 6.0x10^4, and 9.0x10^4, corresponding to wind velocities approximately ranging from 2 m/s to 6 m/s. The glide ratio (Cl/Cd) value acts as the basis for comparing the performance of the airfoils under the environmental conditions prevailing in Shivalik mountain region.

### 2.2. Parameter Selection

#### *2.2.1. Number of Blades for Maximizing the Power Generation*

The blade element theory is a widely used method for analyzing the aerodynamic performance of the blade. According to which, the blade is sub-divided into small micro cells, each of that serves as a distinct blade element. The key aerodynamic properties, including the torque output of the rotor and blade, are calculated once these sub elements are integrated in the direction of its span. Fig. 2 illustrates the nomenclature associated with an aerofoil, where the key attributes play a crucial role in generating a significant portion of both lift and drag. The chord line which connects the trailing and leading edges of the airfoil profile, and the camber line is the curve formed by the points that are midway between the upper and lower surfaces. This configuration induces disturbance in parallel airflow, leading to a pressure disparity, when multiplied by the cross-sectional area it acts upon, generates a force directed towards the low-pressure region [26,27]. Consequently, this force gives rise to an uplifting effect on the body. The "force vector," which is the trigonometric resolution of the combined "lift" and "drag" forces, is divided into two halves in Fig. 3: one perpendicular to the undisturbed "relative wind" direction for lift and one parallel to it for drag. It makes use of Bernoulli's principle that states,

when motion caused by an airfoil profile in wind, generates a response force F by the velocity difference of wind on the blade's surface. The two components of this reaction force are the drag force (D), which acts parallel to the entering velocity V, and the lift force L, which acts perpendicular to the incoming velocity V. The equation defining the aerodynamic force is given by

$$F = 0.5\rho CSV^2 \tag{1}$$

Where ($\rho$) is the fluid density, (C) is the chord length, (V) is the object speed relative to the fluid, (S) is the related surface area of the object.

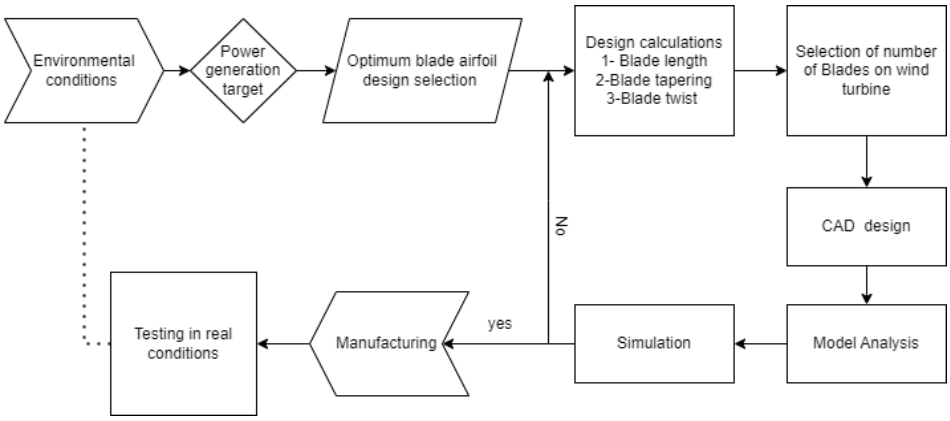


**Fig. 1** Methodology for wind turbine selection

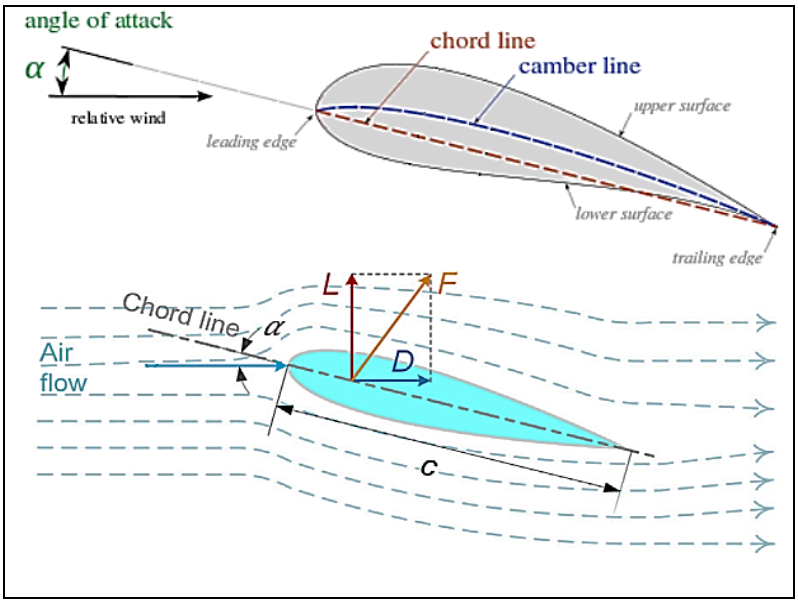


**Fig. 2** Nomenclature of an aerofoil

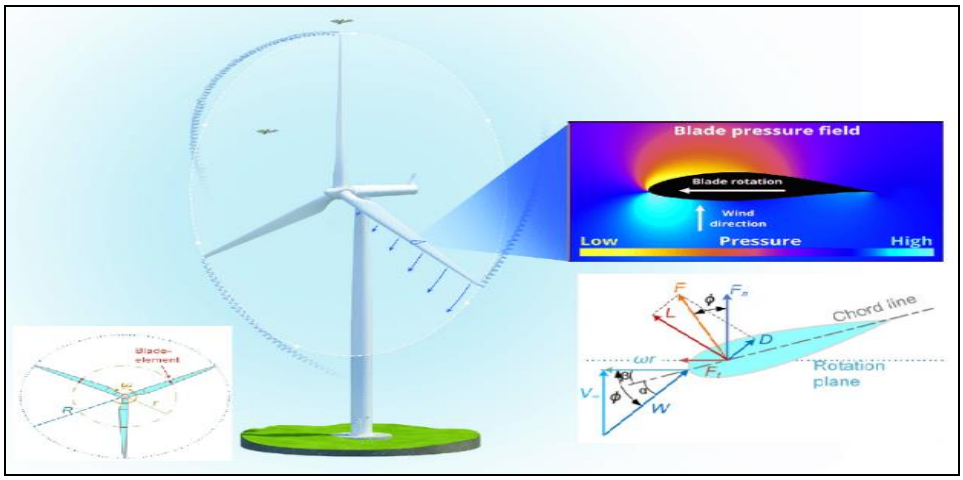


**Fig. 3** Force vector over an airfoil

### 2.3. Lift and Drag

When an airfoil moves through airflow, an aerodynamic force is produced on it, according to Tom Benson's article [24]. The Kutta–Joukowski theorem, which relates lift force (L) and drag force (D) resulting from air circulation around an aerofoil in aerodynamics, is utilised to examine the aerodynamic behaviour of airfoils in dynamic conditions. It provides a foundation for assessing the forces acting on various aerodynamic surfaces, such as wings, rotor blades, and wind turbine blades. The Kutta condition guarantees the consistent airflow at the trailing edge of the aerofoil. Maintaining stable circulation patterns and, thus, constant lift production, depends on this condition. These developments enable the analysis of aerofoils with time-varying movements, such as oscillations or harmonic disturbances, under unstable aerodynamic situations. The theorem considers dynamic impacts in these circumstances, linking the changing circulation patterns to the corresponding modifications.

Any object's lift and drag forces are proportionately determined by the density of fluid wind and relative speed of object to that of wind speed, as the following equation illustrates.

$$L = 0.5\rho cVC_L \tag{2}$$

$$D = 0.5\rho cVC_D \tag{3}$$

Rearranging the Lift equation yields the following equation for the ($C_L$) Lift Coefficient:

$$C_L = \frac{2L}{\rho V^2 A} \tag{4}$$

Where (L) represents the force known as lift , the mass density of wind $(\rho)$, the velocity of wind (v), and (A) is the cross-sectional area. Rearranging the Drag equation yields the following equation for the ($C_D$) Drag Coefficient:

$$C_D = \frac{2D}{\rho V^2 A} \tag{5}$$

where (D represents the force known as drag, or the factor of force in the direction of flow velocity, (A) is the cross-sectional area, (v) is the blade speed in proportion to the wind velocity, and (ρ) is the mass density of the fluid. The torque generated by airflow on the blades varies depending on whether the rotor is horizontal or vertical due to structural and arrangement differences. The horizontal rotor's blade element having delta h thickness that is choosen at distance 'r' from the rotating axis. At this blade element, the tangential velocity $\omega^2 r^2$ and the entering speed V add up to the relative wind speed W, where ω is the angular velocity of the rotor. This relationship is described by the following equation:

$$W = \sqrt{(V^2 + \omega^2 r^2)} \tag{6}$$

Fig. 4 shows the terminology related to an NACA airfoil structure.

The turbine blade profile in this paper uses the NACA four-digit nomenclatures, where first number represents the maximum camber (as percentage of the chord length) shown in Fig. 3, second digit is the maximum camber's distance (from leading edge of the airfoil in tenths of the chord). The final two figures represent the maximum thickness of the airfoil (in percentage of the chord length).

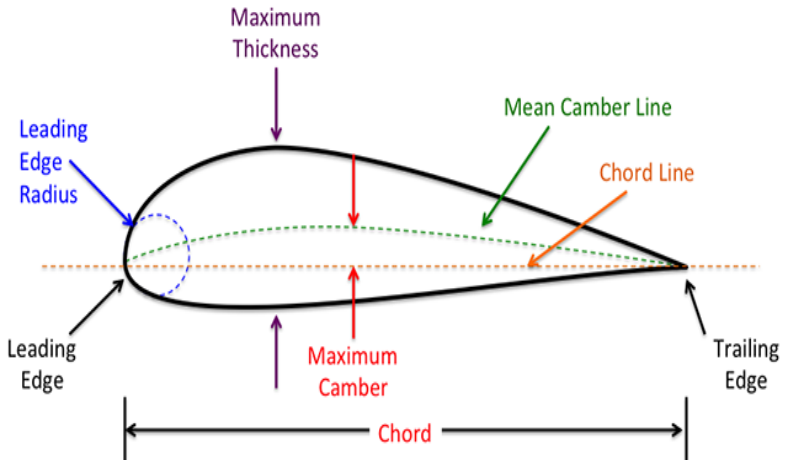


**Fig. 4** NACA airfoil

***Computational Study***

The equation for a symmetrical 4-digit NACA airfoil (NACA 00xx with "xx" being replaced by the percentage of thickness to chord) shape, is

$$y_t = 5t\left[0.2969\sqrt{x} - 0.1260x - 0.3516x^2 + 0.2843x^3 - 0.1015x^4\right] \tag{7}$$

Fig. 5 shows Plots of seven airfoils on the same polar plan diagrams for shape using airfoil tools.

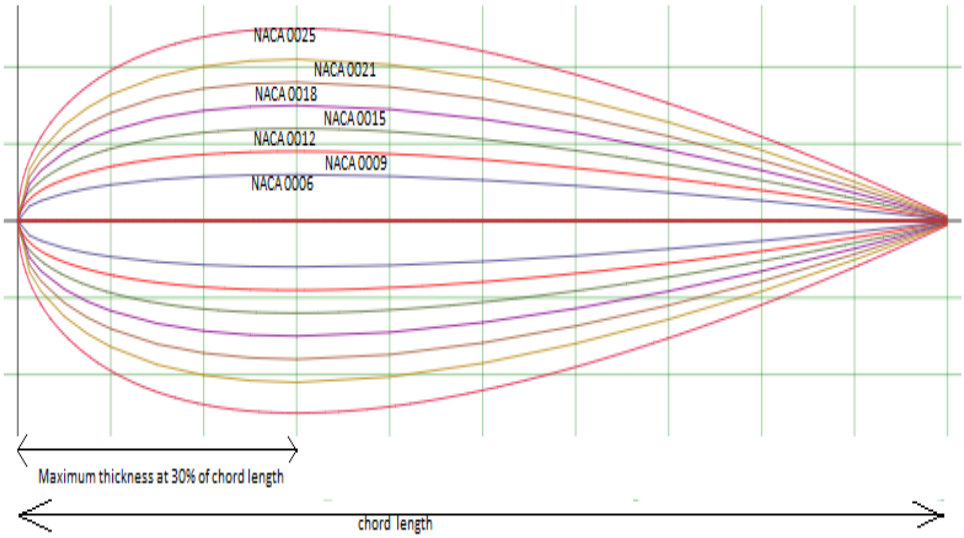


**Fig. 5** Comparision of various airfoil shapes

## 3. Results and Discussion

In the present context of work, multiple airfoils from NACA family were analyzed for different thickness values. Xfoil software is used to analyze and compare the data. Table 1 shows the compiled data generated using xfoil software for numerical comparison between various symmetric airfoils from NACA family over lift, drag and lift to drag ratio with reference to the angle of attack ranging from -8.75 to +10.75 degree. The Reynold number is taken as a fixed value of 10^6.

**Table 1** Symmetrical metrical blades and their characteristics

| NACA Profiles | Maximum thickness % Located at 30 (represented as % of chord length) | Maximum camber (represented as % of chord length) | Location of maximum camber (represented as % of chord length) from the leading edge | Reynold's number | Maximum ratio of lift to drag | Maximum ratio of lift to drag, at angle of attack (in degrees) |
|---|---|---|---|---|---|---|
| 0006 | 6 | 0 | 0 | $10^6$ | 56.6 | 4.5 |
| 0009 | 9 | 0 | 0 | at mac | 74.7 | 8.0 |
| 0012 | 12 | 0 | 0 | speed <1 | 75.6 | 7.5 |
| 0015 | 15 | 0 | 0 | (subsonic | 77.9 | 9 |
| 0018 | 18 | 0 | 0 | speed) | 74.7 | 8.5 |
| 0021 | 21 | 0 | 0 | @Ncrit=9 | 77.9 | 10 |
| 0025 | 25 | 0 | 0 | | 68.9 | 9 |

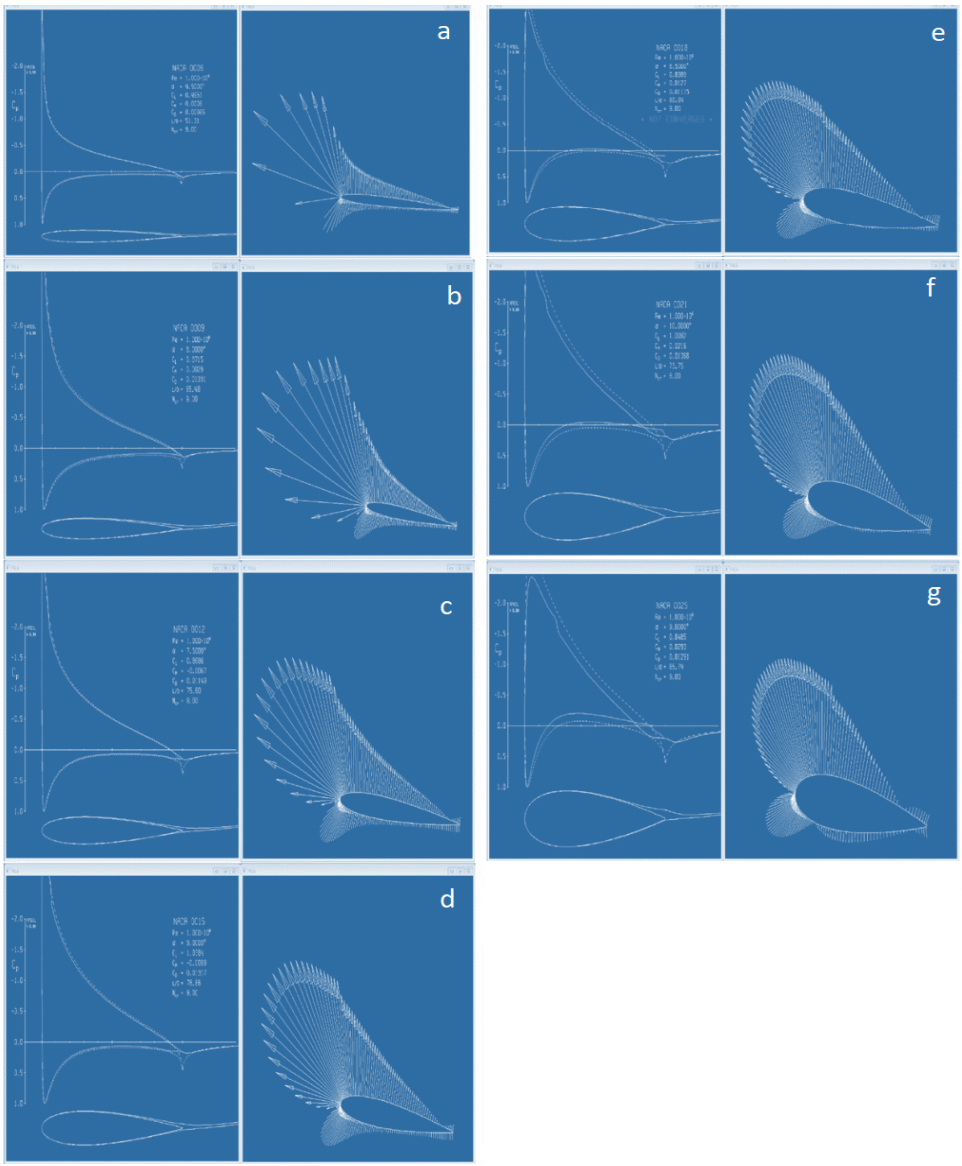


**Fig. 6** Pressure profiling of various blades at maximum lift using xfoil software

Using the maximum lift-to-drag value obtained from the numerical comparison of different profiles at an angle of attack fig 6 is obtained. Fig. 6 (a-g) shows physical comparison of the low-pressure zone at the upper surface of the blade (lift) versus the high-pressure zone at lower surface of the blade (drag) with respect to chord length. Fig 7 (a-g) shows the pressure distribution in comparison with the static stagnant point pressure around NACA airfoil profile blades variation to chord length. The results clearly show

that the top curve near the leading-edge shows lift i.e. suction peak due to accelerated flow around the leading edge profile (increasing kinetic energy and decreased static pressure), while moving towards tail edge kinetic energy decreases due to adverse Pressure gradient and skin friction resulting in minimum static pressure back to free stream or separation from the boundary layer. The lower curve near the leading-edge shows drag pressure i.e. positive pressure due to higher flow mass at lower relative velocity.

The comparison of the coefficient of lift of several NACA airfoils with regard to the angle of attack, which ranges from -8.75 to +10.75 degrees, is displayed in Figure 7. The lift to drag ratios of several NACA airfoils are compared in Fig. 8 with regard to the angle of attack ranging in -8.75 to +10.75 degrees. The results indicate that, when compared to NACA profiles 0006, 0009, 0012, 0015, 0018, 0021, and 0025, NACA 0025 might achieve the highest coefficient of lift. Figure 7 shows that lift-to-drag ratios peaked between 4.5° and 10° of the angle of attack for all airfoils studied. At 4.5° and 10° angles of attack, the NACA 0015 and NACA 0021 airfoils had the highest lift-to-drag ratios of any of them, with respective values of 77.9. The lift coefficients of symmetric airfoils were identical, peaking at similar angles of attack. In particular, the study found that the NACA 0025 airfoil had lift coefficient values of around 1.1959 at an angle of attack of 10.75 degrees and a Reynolds number of 1x10^6. The findings suggest that the pressure differential rises in proportion to the airfoil thickness. Present airfoils appear to be very suitable for low-speed wind turbine symmetric blade construction, particularly at the root section, especially as the pressure differential between the top and lower sides of the airfoil grows. All the results line up with the previous study [27,28] and very suitable for small wind turbine blade designs.

However, the challenge remains with the wind forecasting modeling for better implementation of turbines with such symmetric NACA airfoils due to the lack of self-starting torque generation by such blades at very low speeds [29,30]. Another limitation in the case of micro wind turbines is the wind shadow zones generally found in dense urban city infrastructure micro wind turbines are very helpful in generating electricity in a dense area. Moreover, after sunset these wind turbines even generate electricity in the areas where low wind is available these are special benefits of micro wind technologies.

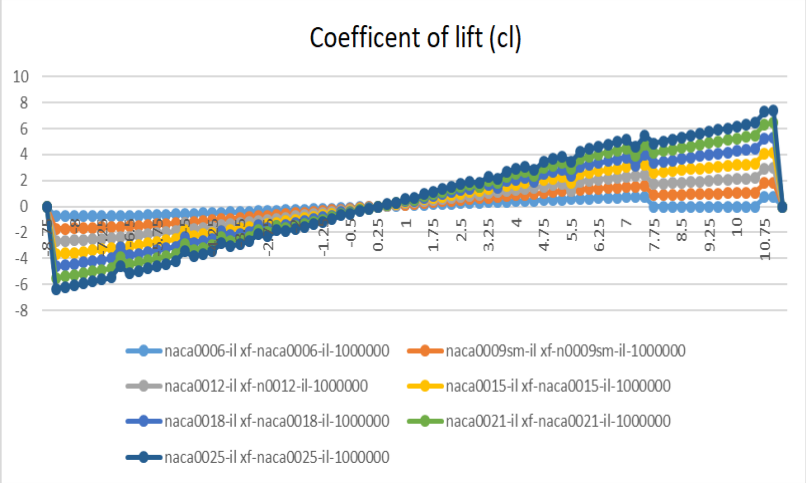


**Fig. 7** Coefficient of lift vs angle of attack

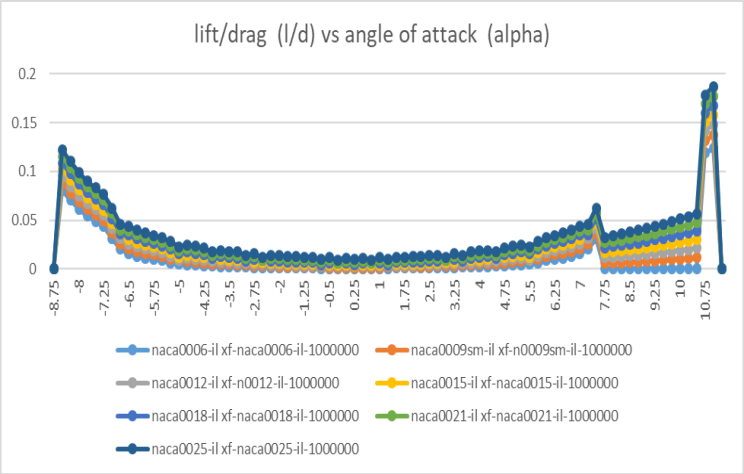


**Fig. 8** Ratio of lift and drag vs angle of attack

## 4. CONCLUSION

In the present work, the aerodynamic performance of seven symmetrical airfoils from the NACA family was analyzed for different thickness values using computational fluid dynamics (CFD) techniques and Xfoil software. The numerical data analyzed was used to obtain the lift coefficient for particular airfoils with angle of attack. Moreover, the maximum lift-to-drag ratio were also obtained for particular airfoils with respect to angle of attack ranging from -8.75 to +10.75 degrees. The comparison of several airfoils reveals that the NACA 0025 maximum coefficient of lift at Re of $10^6$ is 90 degrees of angle of attack and 68.9 lift-to-drag ratio. Although lift-to-drag ratios peaked only within particular angles of attack for all airfoils, the study did find that lift coefficients typically rose with the angle of attack. The CFD results for the NACA airfoils were compared with experimental data mentioned in the report [6], revealing a strong agreement between the numerically simulated and experimentally measured values. Moreover, the lift coefficients calculated through CFD closely matched the data obtained from wind tunnel experiments in the NACA report. The future investigation may include the study to increase the self-starting characteristics of symmetric blades at very low wind speeds by incorporating the various mechanisms like Magnus starter or digital assisted systems to convert classical systems into hybrid systems.

**Funding**: *Himachal Pradesh Council for Science, Technology & Environment (HIMCOSTE) grant no. STC/F(8)-2/2021(R&D)21-22-2053, issued on February 14, 2023, provided funding for this research.*

**Acknowledgment**: *The Himachal Pradesh (H.P.) Council for Science, Technology & Environment (HIMCOSTE) contributed funds to enable the author to carry out this investigation.*

## REFERENCES


[1] United Nations, *Population*, United Nations, 2023. [Online]. Available at: https://www.un.org/en/global-issues/population

[2] IEA, *Global Energy Crisis*, International Energy Agency, 2022. [Online]. Available at: https://www.iea.org/topics/global-energy-crisis

[3] K. Sanjay, S. Sharma, Y. R. Sood, S. Upadhyay and V. Kumar. "A Review on Different Parametric Aspects and Sizing Methodologies of Hybrid Renewable Energy System", *J. Inst. Eng. (India)*, vol. B 103, no. 4, pp. 1345-1354, 2022.

[4] D. Thakur, R. Ganguly and A. K. Gupta, "Characterization and Waste to Energy Techniques for Improving Municipal Solid Waste Management in Una Town, Himachal Pradesh, India – a Case Study", *J. Solid Waste Technol. Manag.*, vol. 46 no. 4, pp. 547-562.

[5] K. Neha, S. Kumar Singh and S. Kumar. "A Review on Performance and Reliability Aspects of Photovoltaic Modules" in *Sustainable Technology and Advanced Computing in Electrical Engineering*, vol. 939, pp. 589-601, Springer Singapore, 2022.

[6] S. Kumar and T. Kaur. "Efficient Solar Radiation Estimation Using Cohesive Artificial Neural Network Technique with Optimal Synaptic Weights", *Proc. Inst. Mech. Eng. A: J. Power Energy*, vol. 234, no. 6, pp. 862-873, 2020.

[7] K. Tarlochan, S. Kumar and R. Segal. "Application of Artificial Neural Network for Short Term Wind Speed Forecasting", In Proceedings of IEEE 2016 Biennial International Conference on Power and Energy Systems: Towards Sustainable Energy (PESTSE), 2016, pp. 1-5.

[8] Y. Ma, A. Zhang, L. Yang, C. Hu and Y. Bai, "Investigation on Optimization Design of Offshore Wind Turbine Blades based on Particle Swarm Optimization", *Energies*, vol. 12, no. 10, pp. 1972-1972, May 2019.

[9] Langley Research Center, *Introduction to the Aerodynamics of Flight*. [Online] Available at: https://ntrs.nasa.gov/api/citations/19760003955/downloads/19760003955.pdf

[10] E. N. Jacobs, K. E. Ward and R. M. Pinkerton, *The Characteristics of 78 Related Airfoil Sections from Tests in the Variable-Density Wind Tunnel*", NASA, Jan. 1933. [Online] Available at: https://ntrs.nasa.gov/api/citations/19930091108/downloads/19930091108.pdf

[11] S. S. Bhat and R. N. Govardhan, "Stall Flutter of NACA 0012 Airfoil at Low Reynolds Numbers", *J. Fluids Struct.*, vol. 41, pp. 166-174, Aug. 2013.

[12] A. A. Matyushenko, E. V. Kotov, A. V. Garbaruk, "Calculations of Flow Around Airfoils Using Two-dimensional RANS: An Analysis of the Reduction in Accuracy", St. Petersbg. Polytech. Univ. J.: Phys. Math., vol. 3, no. 1, pp. 15-21, Mar. 2017.

[13] J. Morgado, R. Vizinho, M. A. R. Silvestre and J. C. Páscoa, "XFOIL vs CFD Performance Predictions for High Lift Low Reynolds Number Airfoils", *Aerosp. Sci. Technol.*, vol. 52, pp. 207-214, May 2016.

[14] K. K. Upender, "Resolving Pitching Airfoil Transonic Aerodynamics by Computational Fluid Dynamics Data Modeling", *J. Fluids Eng.*, vol. 143, no. 9, p. 091501, 2021.

[15] E. N. Jacobs, K. E. Ward and R. M. Pinkerton, *The Characterstics of 78 Related Airfoil Sections from Tests in the Variable Desity Wind Tunnel*. National Advisory Committee for Aeronautics, 1933.

[16] H. J. Goett and W. Kenneth Bullivant. (N.D.). *Tests of N. A. C. A. 0009, 0012, And 0018 Airfoils in the Full Scale Tunnel.* National Advisory Committee for Aeronautics, Langley Memorial Aeronautical Laboratory. National Technical Information Services.

[17] J. V. Booker, *Boundary Layer Transition on the Naca 0012 And 23012 Airfoils in the 8 Foot High Speed Wind Tunnel*. Langley Memorial Aeronautical Laboratory, USA. National Advisory Committee for Aeronautics, USA, 1940.

[18] T. Liu, *Evolutionary Understanding of Airfoil Lift*, 2021.

[19] N. Karthikeyan and T. Suthakar, "Computational Studies on Small Wind Turbine Performance", *J. Phys.: Conf. Ser.*, vol. 759, p. 012087, 2016.

[20] National Renewable Energy Laboratory, *Nrel Airfoil Families For HAWTs*. Colorado: National Technical Information Service (NTIS), U.S. Department of Commerce, Springfield, 1995.

[21] O. Olayemi, O. Ogunwoye and J. Olabemiwo, "Analysis of Flow Characterstics Around an Inclined NACA 0012 Airfoil Using Various Turbulence Models", *IOP Conf. Ser.: Mater. Sci. Eng.*, vol. 1107, p. 012133, 2020.

[22] A. Seeni and P. Rajendran, "Numerical Validation of NACA 0009 Airfoil in Ultra-Low Reynolds Number", Int. Rev. Aerosp. Eng. (IREASE), vol. 12, no. 2, pp. 83-92, 2019.

[23] S. Shukla and Pushparaj Singh, "Computational Analysis of Wind Turbine Blade with Naca 0021 Profile Under High Reynolds Number Using Ansys", *Int. J. Eng. Res. Technol.* (*IJERT*), vol. 6, no. 12, pp. 179-185, Dec. 2017.

[24] T. Benson, *National Aeronautics and Space Administration*, Aerodynamic Forces. [Online] Available at: http://www.grc.nasa.gov/WWW/k12/airplane/presar.html (n.d.)
[25] D. Zhao, D. Shao, and L. Cui, "CTNet: A Data-Driven Time-Frequency Technique for Wind Turbines Fault Diagnosis Under Time-Varying Speeds", *ISA Trans.*, vol. 154, pp. 335-351, 2024.
[26] A. Hasheminezhad, Z. Nazari, B. Yang, H. Ceylan and S. Kim, "A Comprehensive Review of Sustainable Solutions for Reusing Wind Turbine Blade Waste Materials", *J. Env. Manag.*, vol. 366, p. 121735, 2024.
[27] F. Qi, et al, "Maintenance Strategy for Urban Micro Wind Farm Considering Maintenance Route and Resource Allocation", *Appl. Energy*, vol. 377, p. 124515, 2025.
[28] S. Liu, L. Zhang, J. Lu, X. Zhang, K. Wang, Z. Gan, X. Liu, Z. Jing, X. Cui and H. Wang, "Advances in Urban Wind Resource Development and Wind Energy Harvesters", *Renew. Sustain. Energy Rev.*, vol. 207, p. 114943, 2025.
[29] M. Liton Hossain, et al, "Harnessing the Power of Wind: A Comprehensive Analysis of Wind Energy Potential in Dhaka City", *Sustain. Energy Res.*, vol. 11, p. 14, 2024.
[30] M. Liton Hossain, S. M. Nasif Shams and S. Mahmud Ullah, "Harnessing the Power of Wind: A Comprehensive Analysis of Wind Energy Potential in Dhaka City." *Sustain. Energy Res.*, vol. 11, no. 1, p. 14, 2024.